Maximization of acoustic energy difference between two spaces

Mincheol Shin
Institute of Sound and Vibration Research (ISVR), University of Southampton, University Road, Highfield, Southampton S017 1BJ, United Kingdom

Sung Q. Lee[a)]
IT Convergence and Components Laboratory, Nano Convergence Sensor Team, Electronics Telecommunication Research Institute (ETRI), 138 Gajeongno, Yuseong-gu, Daejeon, 305-700, Republic of Korea

Filippo M. Fazi and Philip A. Nelson
Institute of Sound and Vibration Research (ISVR), University of Southampton, University Road, Highfield, Southampton S017 1BJ, United Kingdom

Daesung Kim and Semyung Wang
Department of Mechatronics, Gwangju Institute of Science and Technology (GIST), 261 Cheomdan-gwagiro, Buk-gu, Gwangju, 500-712, Republic of Korea

Kang Ho Park
IT Convergence and Components Laboratory, Nano Convergence Sensor Team, Electronics Telecommunication Research Institute (ETRI), 138 Gajeongno, Yuseong-gu, Daejeon, 305-700, Republic of Korea

Jeongil Seo
Department of Broadcasting and Telecommunications Media Research, Electronics Telecommunication Research Institute (ETRI), 138 Gajeongno, Yuseong-gu, Daejeon, 305-700, Republic of Korea

(Received 4 June 2009; revised 1 May 2010; accepted 8 May 2010)

There has recently been an increasing interest in the generation of a sound field that is audible in one spatial region and inaudible in an adjacent region. The method proposed here ensures the control of the amplitude and phase of multiple acoustic sources in order to maximize the acoustic energy difference between two adjacent regions while also ensuring that evenly distributed source strengths are used. The performance of the method proposed is evaluated by computer simulations and experiments with real loudspeaker arrays in the shape of a circle and a sphere. The proposed method gives an improvement in the efficiency of radiation into the space in which the sound should be audible, while maintaining the acoustic pressure difference between two acoustic spaces. This is shown to give an improvement of performance compared to the contrast control method previously proposed. © *2010 Acoustical Society of America.* [DOI: 10.1121/1.3438479]

PACS number(s): 43.38.Hz, 43.38.Md, 43.60.Fg [AJZ] Pages: 121–131

I. INTRODUCTION

There has been considerable research into the "active control of sound"[1] both for controlling unwanted noise and for producing a desired sound field. In the second case, arrays of sound sources controlled by various beamforming methods[2,3] have been commonly used to generate a desired far field directivity pattern. Such arrays were also investigated by Druyvesteyn and Garas[4] with the objective of producing adjacent regions of audibility and inaudibility. With the objective of using multiple acoustic sources to generate a sound field which audible in one region and inaudible in another, Choi and Kim[5] introduced the concept of regions referred to respectively as a "bright zone," with high acoustic energy, and a "dark zone" where the acoustic energy is low. In their research, two methods are described–one is to maximize the energy in the bright zone with given input source power and the other maximizes the ratio between energies in the bright and dark zone. Much of the previous research has been focused on the development of personal audio systems[4,6] where the intention is to generate a field that is audible to one listener but inaudible to nearby listeners. Recently, for example, a practical implementation of a personal audio system, a so called "active headrest," has been introduced by Elliott and Jones.[6] In addition, a sound focused personal audio system using acoustic contrast control has been realized by Chang *et al.*[7]

This work considers the generation of a sound field that maximizes the energy difference between two spatial regions. The proposed method ensures the control of the amplitude and phase of multiple sources in order to maximize the acoustic energy difference between two selected acoustic spaces. This method also makes use of a "tuning factor" to adjust the balance between two important performance measures; the acoustic energy difference and the efficiency of

[a)]Author to whom correspondence should be addressed. Electronic mail: hermann@etri.re.kr

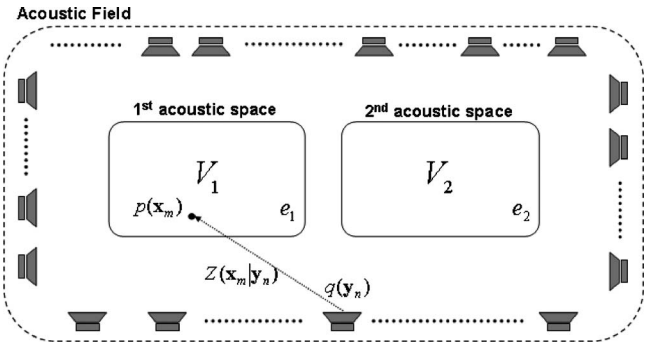

FIG. 1. Definitions of acoustic parameters in an acoustic field: V_1 and V_2 are the volumes of the first and second acoustic spaces, $q(\mathbf{y}_n)$ is the source with volume velocity at the location $\mathbf{y}_n$, $p(\mathbf{x}_m)$ is the pressure at $\mathbf{x}_m$ in acoustic spaces, and $Z(\mathbf{x}_m|\mathbf{y}_n)$ is the acoustic transfer function from the source at $\mathbf{y}_n$ to the pressure point in acoustic space at $\mathbf{x}_m$.

radiation of multiple acoustic sources into the first acoustic space in which sound should be audible. Similarly to the method adopted by Choi and Kim,[5] it is assumed that the sound field is generated by multiple monopole sources. In this paper, we will refer to Choi and Kim's method as "acoustic contrast maximization" while the method proposed here involves "acoustic energy difference maximization." The main difference between the two methods is that Choi and Kim's[5] acoustic contrast is the *ratio* of the mean square pressures between bright and dark zones, while the method proposed here focuses on the *difference* between the mean square pressures between the two acoustic spaces. These two approaches are investigated and compared using simulations and practical experiments. It is shown that the proposed method can give an improved performance for the efficiency of radiation into the space in which the sound should be audible while maintaining the acoustic pressure difference between two acoustic spaces. The proposed method also requires simpler computations (which also avoids ill-conditioning problems) than those associated with the conventional acoustic contrast control method. In addition, the required source strengths are distributed evenly among the sources so that physical realization of the system requires loudspeakers of lower maximum capacity.

This paper begins with the definition of the given acoustic problem. Free-field monopole simulations based on the theoretical formulation are used to verify that the proposed method can produce good performance. Experiments are undertaken in an anechoic chamber and enable a realistic evaluation of the method. A system comprising an array of 40 loudspeakers arranged on a sphere was used in the experimental work. All of the theoretical formulation, simulations and experiments of the proposed acoustic energy difference method are compared with the previously proposed acoustic contrast control method.

II. PROBLEM DEFINITION

Figure 1 describes the concept of the proposed control scheme. The volumes of the two acoustic spaces, between which the difference of acoustic energy is to be maximized, are represented as V_1 and V_2. Even if the design of the acoustic spaces influences the direction of sound, it is not investigated in this paper. The final goal of the control method is to reproduce audible sound in the first acoustic space while maintaining silence in the second acoustic space. The complex magnitude of pressure at position $\mathbf{x}_m$ in the first acoustic space represented by $p(\mathbf{x}_m)$ $(m=1,\ldots,M)$ is assumed to have a time dependence of $e^{j\omega t}$. The volume velocities (source strengths) of the sources at $\mathbf{y}_n(n=1,\ldots,N)$, are denoted by $q(\mathbf{y}_n)$. The acoustic transfer function between the source at $\mathbf{y}_n$ and the pressure at $\mathbf{x}_m$ is described as $Z(\mathbf{x}_m|\mathbf{y}_n)$. Consequently, the pressure vector, $\mathbf{p}^T=[p(\mathbf{x}_1)\ \ p(\mathbf{x}_2)\ \ \cdots\ \ p(\mathbf{x}_M)]$ can be related to the source strength vector, $\mathbf{q}^T=[q(\mathbf{y}_1)\ \ q(\mathbf{y}_2)\ \ \cdots\ \ q(\mathbf{y}_N)]$ by

$$\mathbf{p}=\mathbf{Z}\mathbf{q}, \tag{1}$$

where the matrix of transfer functions is defined by

$$\mathbf{Z}=\begin{bmatrix} Z(\mathbf{x}_1|\mathbf{y}_1) & Z(\mathbf{x}_1|\mathbf{y}_2) & \cdots & Z(\mathbf{x}_1|\mathbf{y}_N) \\ Z(\mathbf{x}_2|\mathbf{y}_1) & Z(\mathbf{x}_2|\mathbf{y}_2) & \cdots & Z(\mathbf{x}_2|\mathbf{y}_N) \\ \vdots & \vdots & & \vdots \\ Z(\mathbf{x}_M|\mathbf{y}_1) & Z(\mathbf{x}_M|\mathbf{y}_2) & \cdots & Z(\mathbf{x}_M|\mathbf{y}_N) \end{bmatrix}.$$

With this notation, the magnitude squared of the complex pressure which is proportional to the acoustic energy density is written as

$$e_1=\frac{1}{V_1}\int_{V_1} p(\mathbf{x})^* p(\mathbf{x})dV_1(\mathbf{x}). \tag{2}$$

When the volume V_1 is approximated by discrete samples which are closely spaced compared to the wavelength of the sound, the volume integral can be represented by the discrete summation using the matrix combination as shown in Eq. (3). Thus,

$$\begin{aligned} e_1 &\cong \frac{1}{M}\sum_{k=1}^{M} p(\mathbf{x}_k)^* p(\mathbf{x}_k)=\frac{1}{M}\sum_{k=1}^{M}(\mathbf{Z}_k\mathbf{q})^*(\mathbf{Z}_k\mathbf{q}) \\ &=\mathbf{q}^H\left(\frac{1}{M}\sum_{k=1}^{M}\mathbf{Z}_k{}^H\mathbf{Z}_k\right)\mathbf{q}=\mathbf{q}^H\mathbf{R}_1\mathbf{q}, \end{aligned} \tag{3}$$

where $p(\mathbf{x}_k)=\mathbf{Z}_k\mathbf{q}$ and $\mathbf{Z}_k=[Z(\mathbf{x}_k|\mathbf{y}_1)Z(\mathbf{x}_k|\mathbf{y}_2)\cdots Z(\mathbf{x}_k|\mathbf{y}_N)]$ which means the kth row of the matrix $\mathbf{Z}$ and * denotes the complex conjugate and H denotes the complex conjugate transpose. The matrix $\mathbf{R}_1=\frac{1}{M}\sum_{k=1}^{M}\mathbf{Z}_k{}^H\mathbf{Z}_k$ can be interpreted as the spatially averaged correlation matrix of transfer functions defined on the sampled points in the first acoustic space. The individual correlation matrix of transfer functions, $\mathbf{Z}_k{}^H\mathbf{Z}_k$ is represented by

$$\mathbf{Z}_k{}^H\mathbf{Z}_k=\begin{bmatrix} Z^*(\mathbf{x}_k|\mathbf{y}_1)Z(\mathbf{x}_k|\mathbf{y}_1) & \cdots & Z^*(\mathbf{x}_k|\mathbf{y}_1)Z(\mathbf{x}_k|\mathbf{y}_N) \\ \vdots & \ddots & \vdots \\ Z^*(\mathbf{x}_k|\mathbf{y}_N)Z(\mathbf{x}_k|\mathbf{y}_1) & \cdots & Z^*(\mathbf{x}_k|\mathbf{y}_N)Z(\mathbf{x}_k|\mathbf{y}_N) \end{bmatrix}. \tag{4}$$

Consequently, the acoustic energy in each acoustic space can be represented respectively by

$$e_1 = \mathbf{q}^H \mathbf{R}_1 \mathbf{q}, \quad e_2 = \mathbf{q}^H \mathbf{R}_2 \mathbf{q}, \tag{5}$$

where $\mathbf{R}_2$ is the spatially averaged correlation matrix in the second acoustic space. In addition, the energy of all the sources is represented by $e_q = \mathbf{q}^H \mathbf{q}$.

III. CONTROL METHODS

A. Acoustic contrast maximization

The proposed acoustic energy difference maximization method, is compared with Choi and Kim's[5] acoustic contrast maximization method. When the spaces in which the sound field is audible and inaudible correspond to the first and second acoustic spaces in Fig. 1 respectively, the cost function to be maximized in the acoustic contrast maximization method can be expressed by

$$J_c(\mathbf{q}) = \frac{e_1}{e_1 + e_2} = \frac{\mathbf{q}^H \mathbf{R}_1 \mathbf{q}}{\mathbf{q}^H (\mathbf{R}_1 + \mathbf{R}_2)\mathbf{q}}, \tag{6}$$

which can be rewritten as

$$\mathbf{q}^H (\mathbf{R}_1 + \mathbf{R}_2)\mathbf{q} J_c(\mathbf{q}) = \mathbf{q}^H \mathbf{R}_1 \mathbf{q}. \tag{7}$$

The source strength vector $\mathbf{q}$ which makes the cost function $J_c(\mathbf{q})$ maximum can be obtained by the partial derivative of Eq. (7) with respect to the source strength vector $\mathbf{q}$. This is given by

$$\frac{\partial J_c(\mathbf{q})}{\partial \mathbf{q}} \mathbf{q}^H (\mathbf{R}_1 + \mathbf{R}_2)\mathbf{q} + J_c(\mathbf{q}) \frac{\partial}{\partial \mathbf{q}} (\mathbf{q}^H (\mathbf{R}_1 + \mathbf{R}_2)\mathbf{q}) = \frac{\partial}{\partial \mathbf{q}} (\mathbf{q}^H \mathbf{R}_1 \mathbf{q}). \tag{8}$$

The optimized source strength vector $\mathbf{q}_c$ makes the cost function $J_c(\mathbf{q})$ extreme, such that $\partial J_c(\mathbf{q})/\partial \mathbf{q} = 0$, and using the gradient property with respect to a complex vector parameter[8] Eq. (8) can be rewritten as $J_c(\mathbf{q}_c)((\mathbf{R}_1 + \mathbf{R}_2)\mathbf{q}_c)^* = (\mathbf{R}_1 \mathbf{q}_c)^*$. Consequently, it follows that

$$J_c(\mathbf{q}_c)\mathbf{q}_c = (\mathbf{R}_1 + \mathbf{R}_2)^{-1} \mathbf{R}_1 \mathbf{q}_c. \tag{9}$$

Equation (9) has the same form as a generalized eigenvector and eigenvalue problem written as $\lambda \mathbf{q}_c = \mathbf{A}\mathbf{q}_c$ where, $J_c(\mathbf{q}_c)$ and $(\mathbf{R}_1 + \mathbf{R}_2)^{-1}\mathbf{R}_1$ are replaced by the eigenvalue λ and the matrix $\mathbf{A}$ respectively. Consequently, the optimized source strength vector $\mathbf{q}_c$ is the eigenvector of the matrix $(\mathbf{R}_1 + \mathbf{R}_2)^{-1}\mathbf{R}_1$ that corresponds to the largest eigenvalue and the maximum of the cost function, $J_c(\mathbf{q}_c)$.[9] Clearly, the optimum solutions to Eq. (9) are frequency dependant.

B. Acoustic energy difference maximization

There is a crucial conceptual limitation associated with the cost function of the acoustic contrast maximization method. The maximized contrast, which implies maximized energy "ratio" between two spaces, cannot always provide the desirable optimum solution which has the maximum numerator and the minimum denominator. The maximization of contrast tries to find the minimum denominator which most readily maximizes the cost function even if the numerator has a very small value.

A good alternative cost function is provided here to overcome this limitation. The basic concept for the cost function proposed here is not the "ratio" but the "difference" between energies of the two acoustic spaces. This is effective simply because the maximized difference implies the maximization of the "minuend" (energy in the first space) and the minimized "subtrand" (energy in the second space).

This is illustrated in Fig. 1 which shows the generation of the maximum sound level in the first acoustic space and minimum level in the second space. The proposed cost function which represents normalized energy difference considering both acoustic energy difference and source energy is written as

$$J_d(\mathbf{q}) = \frac{e_1 - \alpha e_2}{e_q} = \frac{\mathbf{q}^H (\mathbf{R}_1 - \alpha \mathbf{R}_2)\mathbf{q}}{\mathbf{q}^H \mathbf{q}}. \tag{10}$$

A tuning factor α, which is a positive real number, is inserted in the cost function to enable the adjustment of the relative importance between acoustic energy difference and the efficiency of radiation of the multiple sources into the first acoustic space in which the sound should be audible. For example, the maximization problem of the cost function with small α puts more weight on the maximization of the energy in the first acoustic space, $\mathbf{q}^H \mathbf{R}_1 \mathbf{q}$ normalized by the source energy, $\mathbf{q}^H \mathbf{q}$ in Eq. (10). This is in turn related to the efficiency of radiation of the sources into the first acoustic space. On the other hand, the maximization problem of the cost function with large α is weighted more on the minimization problem of the energy in the second acoustic space, $\mathbf{q}^H \mathbf{R}_2 \mathbf{q}$. Consequently, the tuning factor α introduces flexibility into the acoustic energy difference maximization method that allows solutions to be "tuned" considering the energy quantity in the first acoustic space and energy difference between the two spaces. The optimal tuning factor to maximize the acoustic energy difference can be defined using a curve of acoustic energy difference with respect to the tuning factor or by using conventional optimization techniques.[10]

The optimized source strength vector $\mathbf{q}_d$ to maximize the cost function in Eq. (10) can be calculated in the same manner as the acoustic contrast maximization method. The source strength vector $\mathbf{q}_d$ is obtained from the partial derivative of Eq. (10) with respect to the source strength vector $\mathbf{q}$ when the cost function $J_d(\mathbf{q})$ has the extreme value.

$$J_d(\mathbf{q}_d)\mathbf{q}_d = (\mathbf{R}_1 - \alpha \mathbf{R}_2)\mathbf{q}_d. \tag{11}$$

The optimized complex source strength vector $\mathbf{q}_d$ which maximizes the cost function $J_d(\mathbf{q}_d)$ is obtained from the eigenvector of the matrix $\mathbf{R}_1 - \alpha \mathbf{R}_2$ that corresponds to the largest eigenvalue of this matrix.

C. Comparison between acoustic contrast and energy difference maximization

The source strength vector obtained from the acoustic contrast maximization method cannot guarantee that the sound energy in the first acoustic space is audible. In other words, the radiation efficiency, or the ratio between the energy of the sources and the energy in the first acoustic space, is not considered within the cost function in Eq. (6). The

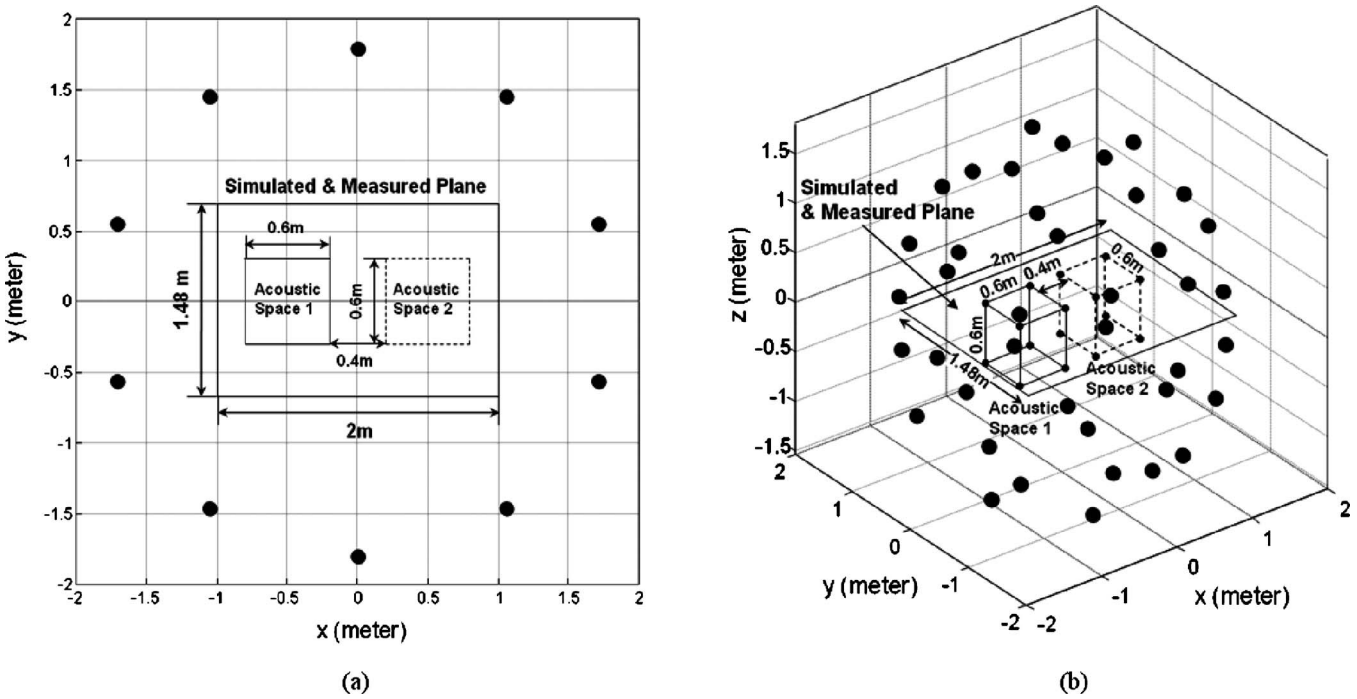

FIG. 2. Simulation configurations: (a) 2–D circular array composed of 10 monopole sources; (b) 3–D spherical array composed of 40 monopole sources with two acoustic spaces located in the middle of the array. Acoustic space 1 is represented by solid line and acoustic space 2 is depicted by dashed lines.

acoustic potential energy of the total zone of interest is the energy sum of the bright zone and the dark zone.[5] Thus the acoustic contrast maximization method only gives the solution for the maximized ratio of energy between the first acoustic space and the total spaces of interest while the sound in the first acoustic space may not be of sufficient amplitude to be audible. However, the acoustic energy difference maximization method ensures that the energy in the first acoustic space is considered in the cost function given by Eq. (10).

There are also advantages of computational efficiency and robustness associated with the energy difference maximization method. Thus the optimum solution for the acoustic contrast maximization method is obtained by the eigenvector corresponding to the largest eigenvalue of $(\mathbf{R}_1+\mathbf{R}_2)^{-1}\mathbf{R}_1$ while the solution of the proposed method is obtained from the largest eigenvalue of $\mathbf{R}_1-\alpha\mathbf{R}_2$. The matrix inversion in the contrast maximization method which has an associated computational burden is replaced by simple matrix subtraction in the energy difference maximization method. Furthermore, if the matrix $(\mathbf{R}_1+\mathbf{R}_2)$ is an ill-conditioned matrix with a large condition number, its inversion can cause comparatively large numerical rounding errors with small errors in the elements of the matrix.[11] The matrix ill-conditioning is caused by not only the zone selection but also by similarity of the elements of the matrices as the transfer functions are similar in case of the low frequencies excitation with large wavelength. In addition, the matrix $\mathbf{R}_1-\alpha\mathbf{R}_2$ preserves the characteristics of Hermitian matrices $\mathbf{R}_1$ and $\mathbf{R}_2$. The eigenvalues of the Hermitian matrices are "perfectly well conditioned"[11] which means any perturbations in the elements of a matrix lead to perturbations in the eigenvalues that are roughly the same size. However, the matrix $(\mathbf{R}_1+\mathbf{R}_2)^{-1}\mathbf{R}_1$ can be ill-conditioned and small perturbations in the matrix can give very large perturbations in the eigenvalues. This is especially critical when the transfer functions are measured with small errors. When the transfer functions are measured with slight errors, they cause large errors in obtaining the optimum solution. Thus the proposed method can provide a good alternative when the correlation matrix of transfer functions is ill-conditioned.

Consequently, the energy difference maximization method provides computational efficiency by replacing the matrix inversion with the matrix subtraction and computational robustness by avoiding matrix ill-conditioning problems.

IV. MONOPOLE SIMULATIONS

All sources used in the simulations are simple free-field monopoles. Consequently, the simulations assume the free-field Green function to be the transfer function which is given by Eq. (12) when the wave number is k and the air density is ρ. Thus

$$Z(\mathbf{x}_m|\mathbf{y}_n)=\frac{j\omega\rho}{4\pi}\frac{e^{-jkD}}{D}, \tag{12}$$

where $D=|\mathbf{x}_m-\mathbf{y}_n|$. All sources radiate single frequency sound at 100, 200, and 300 Hz in the simulations. One of the reasons that the frequencies of interest are limited to 100, 200 and 300 Hz pure tones is to obtain comparable simulation results with experiments using real loudspeakers approximately regarded as monopole sources in the low frequency range below 300Hz. Controllability of the sound field below and above this frequency range is in any case very limited because of the distances from the sound sources to

the acoustic spaces to be controled and the gaps separating the sound sources[3,12] The 2-D circular and 3-D spherical source array simulations have been undertaken to illustrate the performance of the acoustic contrast and energy difference maximization methods. The optimized source strength vectors by the acoustic contrast maximization method are obtained from the cost function in Eq. (6). The resultant source strength vector using the acoustic energy difference maximization method is obtained from the cost function in Eq. (10) with the specified tuning factor α. The value of α is chosen to ensure the maximum spatially averaged sound pressure difference between the two acoustic spaces. All simulation results are obtained with the temporal sampling rate of 48 kHz and the spatial sampling rate of 2 cm intervals. The source strength vectors have been normalized to ensure that $\mathbf{q}^H\mathbf{q}$ is equal to 1 in all cases because all of the results produced by simulations and experiments can be reasonably compared when the overall power of the source strength vector is constant.

A. 2-D circular source array simulation

The configuration of the 2-D circular source array simulation is illustrated in Fig. 2(a) with 10 monopole sources located on the circumference of the circular shape. The two acoustic spaces given by squares of 0.36 m^2 (0.6×0.6 m^2) are located in the middle of 2-D circular source array with 0.4 m separated gap. The size of the acoustic space is chosen to include the size of the human head. The locations of the acoustic spaces are determined to obtain the maximum distance from every loudspeaker in the spherical array. The shortest distance from every loudspeaker to both acoustic spaces is around half of the longest wavelength (3.43 m at 20 °C) of the 100Hz excitation signal with the 0.4 m separated gap determined by considering the size of the simulated and measured plane (2×1.48 m^2). The two maximization control methods (for acoustic contrast and energy difference) are applied to obtain the source strength vectors. The 10 monopole sources in the circular array are shown in Table I with the sources numbered from 17 to 26. The simulated acoustic plane is the rectangular area that includes the two acoustic spaces and matches with the experimented acoustic plane covered by the microphone array. The results of 2-D circular source array simulation are shown in Fig. 3 with a gray scale map which represents the pressure field inside the simulated plane. In the gray scale map, the higher acoustic pressure is depicted as a lighter shade and the lower is darker ranging from 50 dB to 100 dB. Figure 3 shows the comparison between the conventional acoustic contrast maximization method (a, b, c) and the proposed energy difference maximization method (d, e, f) at the three excitation frequencies, 100 Hz in (a), (d), 200 Hz in (b), (e), and 300 Hz in (c), (f).

B. 3-D spherical source array simulation

The 3-D simulation configuration is shown in Fig. 2(b) with 40 monopole sources located on the surface of a sphere. The two acoustic spaces given by the cubes of 0.216 m^3 ($0.6 \times 0.6 \times 0.6$ m^3) including the size of a human head are located in the center of spherical source array with 0.4 m gap. Table I gives all of the coordinates of the monopole sources. The simulated acoustic plane described in Fig. 2(b) is the same as that for the 2-D circular array configuration shown in Fig. 2(a). For the simulation arrangement shown in Fig. 2(b), the optimized source strength vectors are again derived from the two maximization control methods. The results are shown in Fig. 4, which represents the acoustic pressure field within the simulated plane as gray scale maps on a decibel scale.

TABLE I. Coordinates of sources in the 3D spherical array simulation and experimental setup when the center of the sphere is set as the origin $(x,y,z)=(0,0,0)$. The sources numbered from 17 to 26 are used in the 2D circular array simulation and experimental setup.

	Coordinate (m)		
Source No.	x	y	z
1	0	0	1.8
2	0.9463	0	1.5312
3	0.2924	0.9	1.5312
4	−0.7656	0.5562	1.5312
5	−0.7656	−0.5562	1.5312
6	0.2924	−0.9	1.5312
7	1.61	0	0.805
8	1.2387	0.9	0.9463
9	0.4975	1.5312	0.805
10	−0.4732	1.4562	0.9463
11	−1.3025	0.9463	0.805
12	−1.5312	0	0.9463
13	−1.3025	−0.9463	0.805
14	−0.4732	−1.4562	0.9463
15	0.4975	−1.5312	0.805
16	1.2387	−0.9	0.9463
17	1.7119	0.5562	0
18	1.058	1.4562	0
19	0	1.8	0
20	−1.058	1.4562	0
21	−1.7119	0.5562	0
22	−1.7119	−0.5562	0
23	−1.058	−1.4562	0
24	0	−1.8	0
25	1.058	−1.4562	0
26	1.7119	−0.5562	0
27	1.5312	0	−0.9463
28	1.3025	0.9463	−0.805
29	0.4732	1.4562	−0.9463
30	−0.4975	1.5312	−0.805
31	−1.2387	0.9	−0.9463
32	−1.2387	−0.9	−0.9463
33	−0.4975	−1.5312	−0.805
34	0.4732	−1.4562	−0.9463
35	1.3025	−0.9463	−0.805
36	0.7656	0.5562	−1.5312
37	−0.2924	0.9	−1.5312
38	−0.9463	0	−1.5312
39	−0.2924	−0.9	−1.5312
40	0.7656	−0.5562	−1.5312

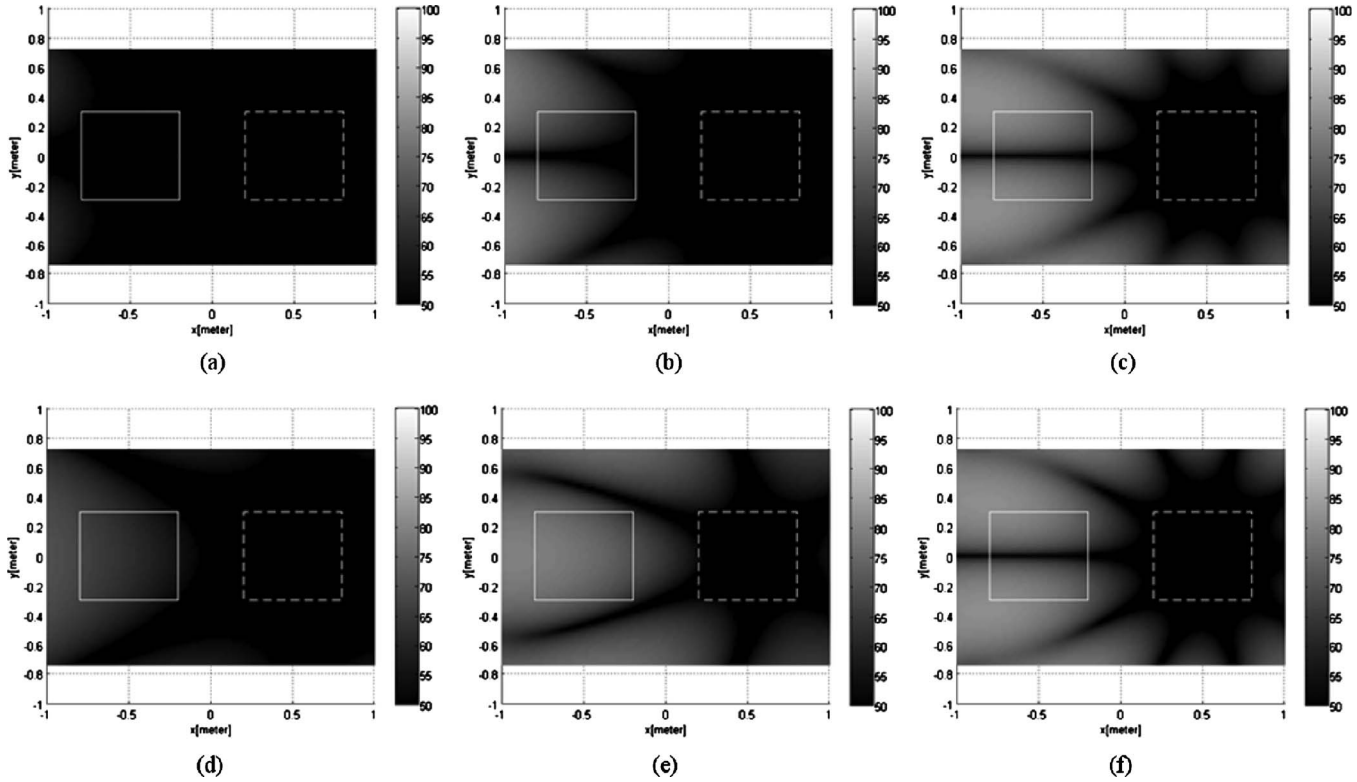

FIG. 3. Simulation results of 2–D circular array. Pressure fields in the simulated plane with sources controlled by the conventional acoustic contrast maximization method ((a), (b), and (c)) and the proposed acoustic energy difference maximization method ((d), (e), and (f)). The excitation frequency for ((a) and (d)) is 100 Hz, 200 Hz for ((b) and (e)), and 300 Hz for ((c) and (f)).

C. Discussions

The performance of the proposed acoustic energy difference maximization method is compared with the conventional acoustic contrast maximization method with three performance measures. The first measure is the efficiency of radiation into the first (audible) spaces. This measures the

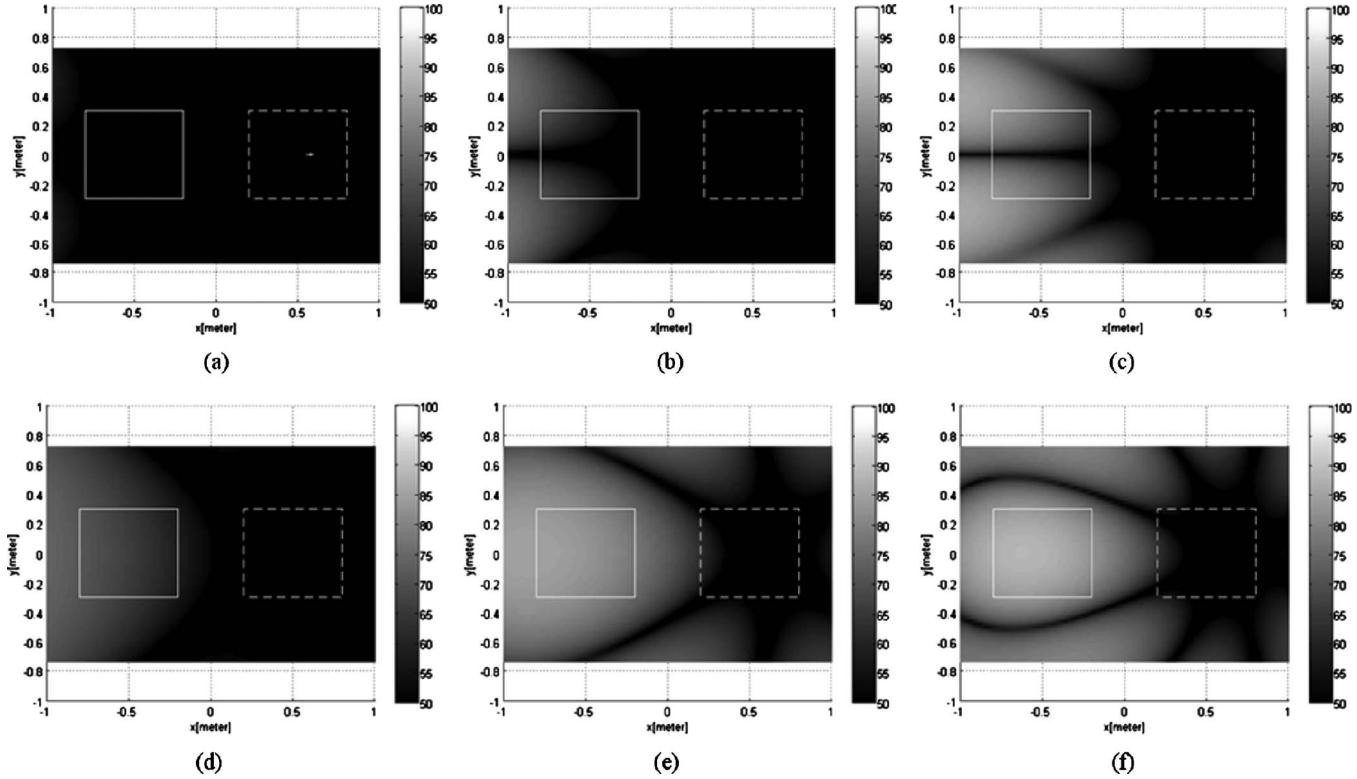

FIG. 4. Simulation results of 3–D spherical array. Pressure fields in the simulated plane with sources controlled by the acoustic contrast maximization method ((a), (b), and (c)) and the proposed acoustic energy difference maximization method ((d), (e), and (f)). The excitation frequency for ((a) and (d)) is 100 Hz, 200 Hz for ((b) and (e)), and 300 Hz for ((c) and (f)).

TABLE II. Results of monopole simulations. AC and AED are abbreviations of Acoustic Contrast and Acoustic Energy Difference maximization methods, respectively. The spatially averaged sound pressure levels in dB scale within each acoustic space denoted as 1 and 2 are listed.

	2–D circular array						3–D spherical array					
	100 Hz		200 Hz		300 Hz		100 Hz		200 Hz		300 Hz	
Applied method	1	2	1	2	1	2	1	2	1	2	1	2
AC	56.5	2.6	78.3	30.3	89.4	49.7	51.7	−12.3	74.4	16.5	89.9	38.8
	$\alpha=987$		$\alpha=330$		$\alpha=1580$		$\alpha=1830$		$\alpha=274$		$\alpha=102$	
AED	76.6	44.6	88.5	59.8	90.0	52.0	81.1	43.3	96.5	63.5	99.5	65.7

spatially averaged sound pressure level in the first acoustic spaces produced by the same source power. This shows that the sound radiated from the sources is audible in the first space. The second measure is the spatially averaged sound pressure level difference on a dB scale between the two acoustic spaces. It gives an important measure for generating the wanted sound field, described in Sec. II, when the first measure has a sufficient value. The third measure is the standard deviation of the magnitude of the source strength vector, which is directly related with the dynamic range of the loudspeakers implemented in real applications.

For the 2-D and 3-D simulations described above, the performance of the proposed acoustic energy difference maximization method is compared with that of the conventional acoustic contrast maximization method. As shown in Figs. 3 and 4, the proposed energy difference method produces a higher acoustic pressure from the sources to the first acoustic space than the case when using the contrast control method. It is because the energy difference can always be maximized when the energy in the audible space is maximized, while the energy contrast can be maximized only with the maximized ratio without consideration of the energy in the audible space. Table II shows a comparison between the two methods for the results of the monopole simulations. The first criterion shows the spatially averaged sound pressure level for each acoustic space on a dB scale. For the efficient representation of the sound pressure level within a certain acoustic space, the spatially averaged sound pressure level is defined as,

$$L_V = 10 \cdot \log_{10}\left(\frac{1}{V}\int_V \frac{|p_V|^2}{p_{\text{ref}}^2} dV\right) \cong 10 \cdot \log_{10}\left(\frac{1}{M}\sum_{k=1}^{M} \frac{|p(\mathbf{x}_k)|^2}{p_{\text{ref}}^2}\right), \quad (13)$$

where V is the volume of the selected acoustic space and p_V is the pressure in the space while p_{ref} means the reference sound pressure of 20 μPa. The volume integral can be represented with the discrete summation where the number of samples in the acoustic space is M and the pressure is depicted as $p(\mathbf{x}_k)$ at the location of $\mathbf{x}_k$. This is identically defined in both simulation and experiment. From the spatially averaged sound pressure levels in Table II, the proposed method always gives higher pressure values in the first acoustic space which implies a better efficiency of radiation to the audible region for normalized $\mathbf{q}$.

Based on Table II, as the performance measure, the spatially averaged acoustic pressure levels of two acoustic spaces with respect to the contrast and difference maximization control methods are represented on a dB scale in Fig. 5. In the case of the contrast maximization method, the spa-

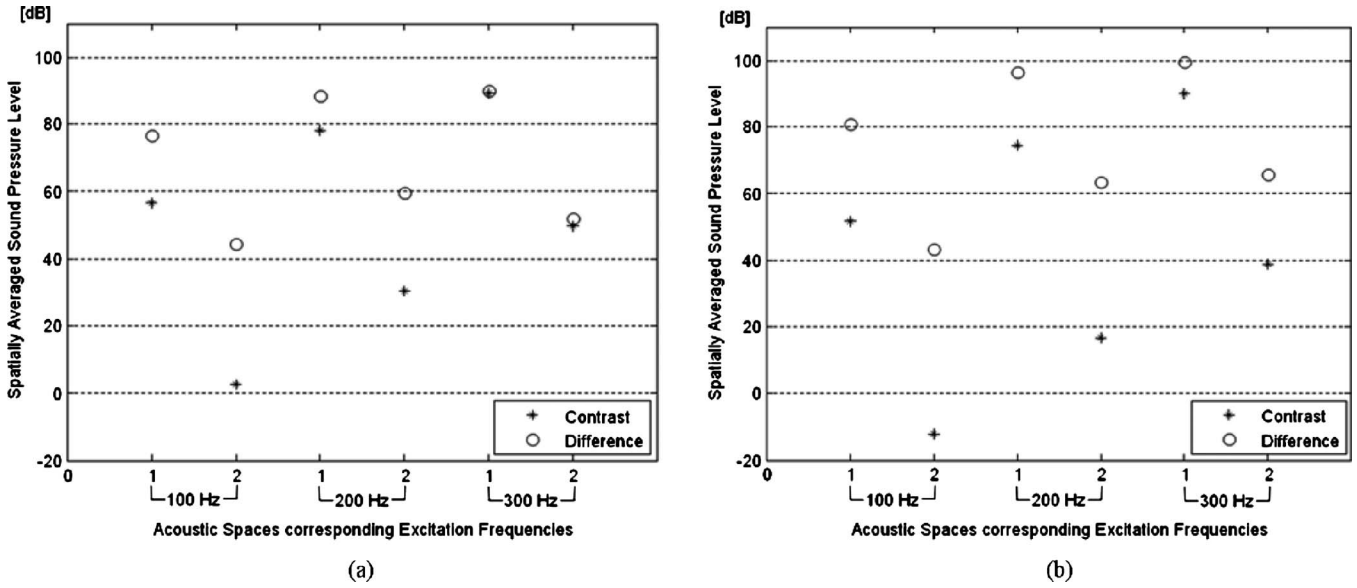

FIG. 5. Spatially averaged acoustic pressure level of two acoustic spaces corresponding to the excitation frequencies based on Table II in case of (a) circular and (b) spherical arrays (*: acoustic contrast maximization method, °: acoustic energy difference maximization method).

TABLE III. Standard deviations of the magnitudes of the obtained source strength vectors.

	2–D circular array			3–D spherical array		
Applied method	100 Hz	200 Hz	300 Hz	100 Hz	200 Hz	300 Hz
AC	0.23	0.21	0.20	0.14	0.13	0.13
AED	0.13	0.15	0.18	0.09	0.05	0.05

tially averaged sound pressure level differences on a dB scale, which means the ratio, between the two acoustic spaces are always higher than those produced by the acoustic energy difference maximization method. However, the spatially averaged sound pressure levels in the first spaces under the control of acoustic energy difference maximization are always higher than those under the contrast control method although the power summations of the controlled source strengths in both methods are set at unity. Therefore, the efficiency of radiation into the first (audible) acoustic spaces is higher when the proposed acoustic energy difference maximization control method is applied. In addition, it maintains the pressure differences between two acoustic spaces at more than 30 dB.

Table III shows the standard deviations of the magnitudes of the source strength vectors with respect to frequency as the performance measure which is defined as,

$$\sigma = \sqrt{\frac{1}{N}\sum_{k=1}^{N}\left(|q(\mathbf{y}_k)| - \frac{1}{N}\sum_{n=1}^{N}|q(\mathbf{y}_n)|\right)^2}. \tag{14}$$

It represents the magnitude range of controlled source signals which are directly related to the dynamic range of the loudspeakers used. If this performance measure has a larger value, the multiple source signals with larger magnitude deviation are applied so that it makes the real implementation more costly. From the results in Table III, the proposed acoustic energy difference maximization method always gives a smaller value of the standard deviations of source strength magnitudes than the contrast maximization method. It is also much smaller in case of the spherical array case than the circular one.

With the results from the performance measures described above, the proposed acoustic energy difference maximization method gives higher efficiency of radiation into the first acoustic space, in which sound should be audible, and maintains more than 30dB pressure difference between the first and second spaces even if it has a smaller value of standard deviation for the magnitudes of controlled source signals.

V. EXPERIMENTS

The experimental arrangement shown in Fig. 6 was constructed in an anechoic chamber in order to validate the 3-D free-field sound generation[13] and the performance of the control methods. The experiments were undertaken for both 2-D circular and 3-D spherical arrangements corresponding to the equivalent simulations. For the 2-D circular array experiment, only 10 loudspeakers in the center circle are activated while all 40 loudspeakers are used for the 3-D spherical array. In correspondence with the monopole simulation, the sampling rate adopted is 48 kHz for all of the signals to the loudspeakers. The loudspeaker locations are described by the coordinates of Table I. The radiation pattern of each loudspeaker used in these experiments has been measured and reported by Fazi *et al.*,[14,15] and are similar to that of a monopole source in the frequency range of interest from 100 to

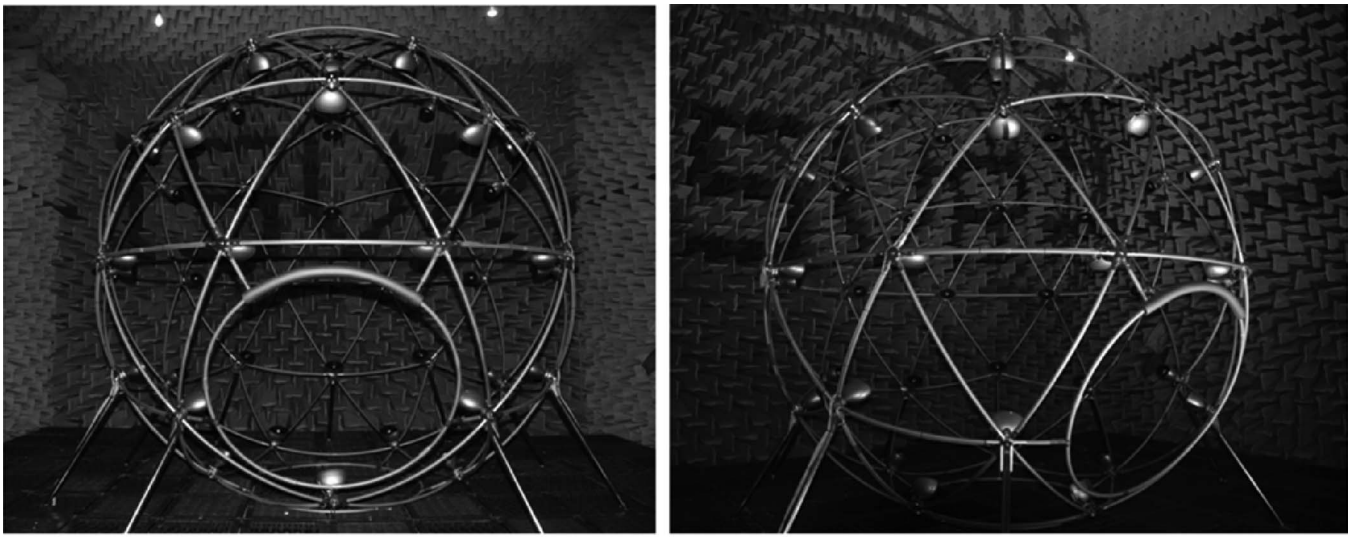

(a) (b)

FIG. 6. Experimental setup in an anechoic chamber composed of 40 loudspeakers with spherical array (a) front and (b) side views.

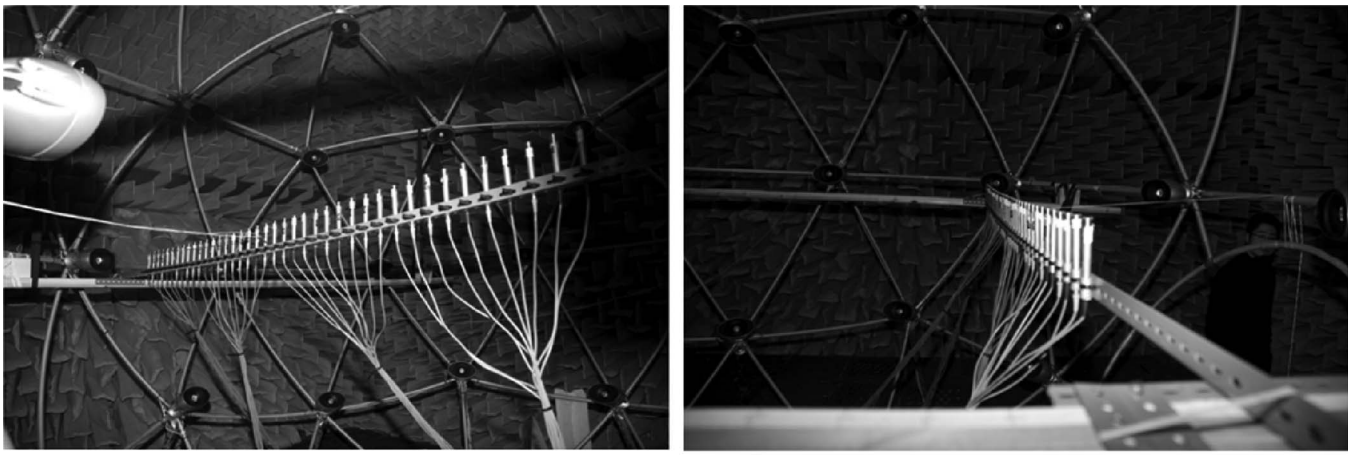

(a) (b)

FIG. 7. Measurement setup with linear array composed of 30 condenser microphones: (a) front and (b) side views.

300 Hz. It is thus expected that the monopole assumption in the simulations is broadly applicable in these real experiments.

In addition, as shown in Fig. 7, the experimental results are measured by 30 equally distributed microphones in a line array inside the spherical experimental arrangement. The gap between two adjacent microphones is 0.051 m which is sufficient to avoid spatial aliasing for frequencies of interest so that the total microphone array length is 1.48 m. The line microphone array is moved at discrete intervals of 0.05 m over 2 m to measure a sufficient area which includes the audible and inaudible acoustic spaces. In Figs. 2(a) and 2(b), the planes measured by the microphone array are depicted and compared with the same simulated plane. The pressure fields are measured with the same temporal sampling rate as those of the source signals.

Figures 8 and 9 show the results of the measured pressure fields of real 2-D and 3-D experiments. The acoustic contrast maximization method and the proposed energy difference maximization method are again compared at the frequencies of 100, 200, and 300 Hz. The results of experiments are very similar to those of simulations in the form of the pressure distributions since the assumptions regarding the free field radiation of the monopole sources are very nearly

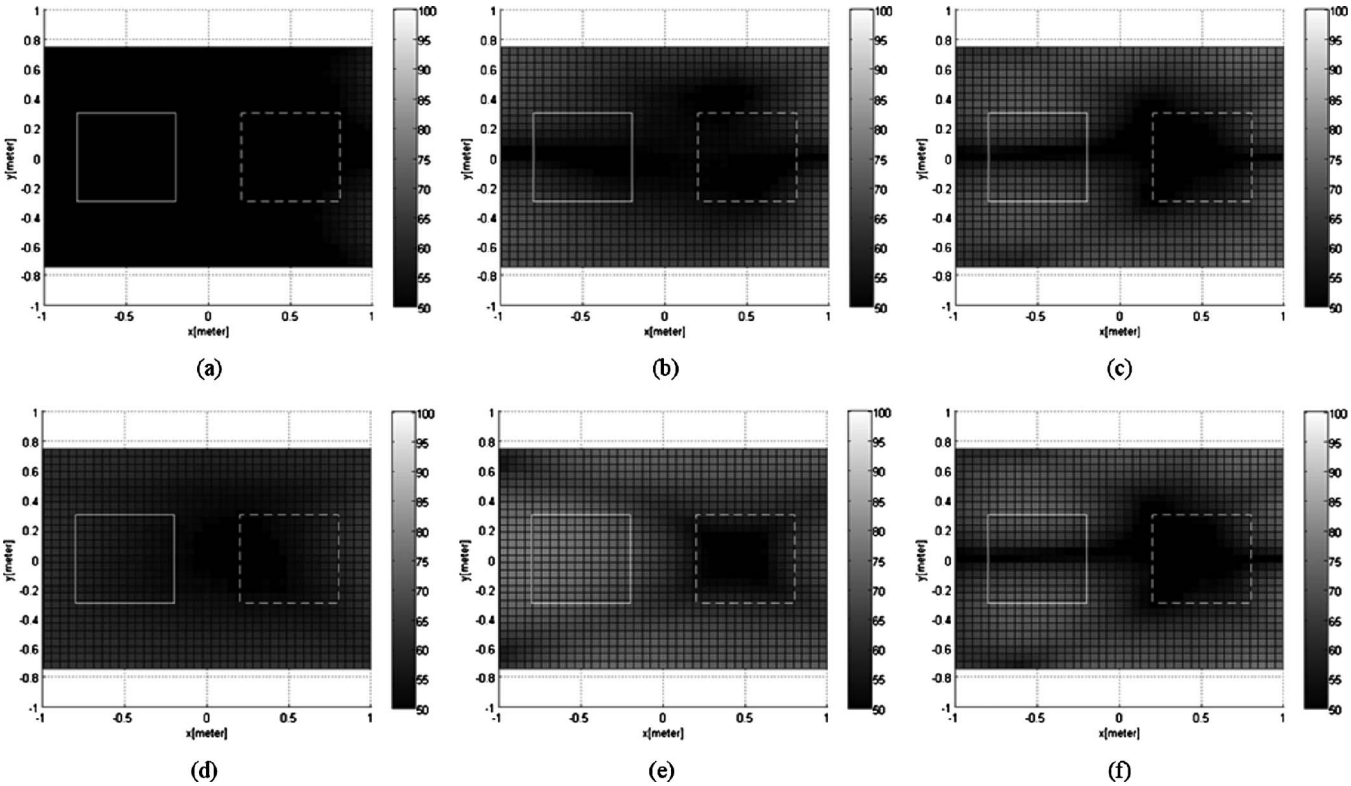

FIG. 8. Experimental results of 2–D circular array. Pressure fields in the measured plane with sources controlled by the acoustic contrast maximization method ((a), (b), and (c)) and the proposed acoustic energy difference maximization method ((d), (e), and (f)). The excitation frequency for ((a) and (d)) is 100 Hz, 200 Hz for ((b) and (e)), and 300 Hz for ((c) and (f)).

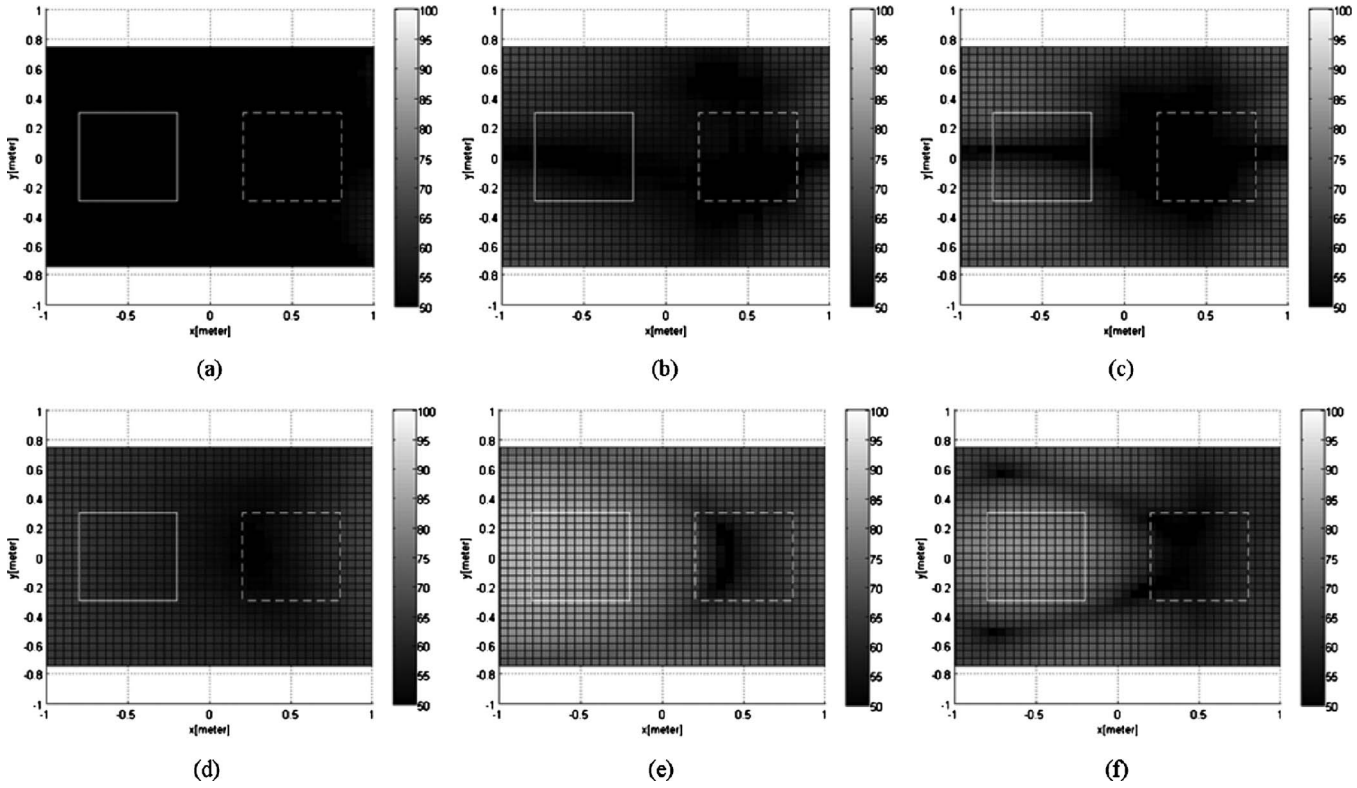

FIG. 9. Experimental results of 3–D spherical array. Pressure fields in the measured plane with sources controlled by the conventional acoustic contrast maximization method ((a), (b), and (c)) and the proposed acoustic energy difference maximization method ((d), (e), and (f)). The excitation frequency for ((a) and (d)) is 100 Hz, 200 Hz for ((b) and (e)) and 300 Hz for ((c) and (f)).

satisfied in this experiment. However, the equivalent pressure values inside the acoustic spaces are not exactly matched with the simulations due to background noise, the mismatches of the sound source locations between simulation and experimental setups and the mutual mismatches of magnitude and phase of the real loudspeakers. Especially, the performance in the experimental results is highly dependant on the mutual identity of the characteristics of all loudspeakers as well as the individual characteristics of the loudspeakers installed in the array structure. Although the loudspeakers used in the array have acceptable individual characteristics, all of the loudspeakers should be identical in their magnitude and phase response with respect to the frequency range of interest. These can cause the mismatches between the results of simulation and experiment as well as the monopole assumption in the simulation results. In addition, in the case of the contrast control method, it is not easy to achieve agreement with the optimum solution from the theory because slight errors between theory and the real experiment cause large errors due to the ill-conditioned matrix inverse problem. The spatially averaged sound pressure levels, in each acoustic space with each control method, were measured and are listed in Table IV. These results show that the proposed acoustic energy difference maximization method has a desirable performance at the frequencies of interest. As shown in Fig. 10 based on Table IV, the proposed acoustic energy difference maximization method always gives a greater pressure difference between the two spaces and a higher pressure level in the first acoustic space. This implies a better efficiency of radiation from the sources to the audible space, together with evenly distributed source strength vectors shown in Table III which means less costly implementation with real loudspeakers although the experimental results given by the contrast maximization method in Table IV are considerably degraded by comparison with the monopole simulations in Table II due to the limitations of the sound sources.

VI. CONCLUSIONS

A multiple source control method is introduced that enables the maximization of the acoustic energy difference be-

TABLE IV. Results of experiments. The spatially averaged sound pressure levels in dB scale within each acoustic space denoted as 1 and 2 are listed.

	2D circular array						3D spherical array					
	100 Hz		200 Hz		300 Hz		100 Hz		200 Hz		300 Hz	
Applied method	1	2	1	2	1	2	1	2	1	2	1	2
AC	49.2	56.5	68.4	64.8	75.9	65.7	52.7	55.2	66.1	62.7	74.5	62.6
AED	68.3	66.1	84.5	67.3	77.1	64.5	72.4	68.9	95.8	74.0	90.4	67.1

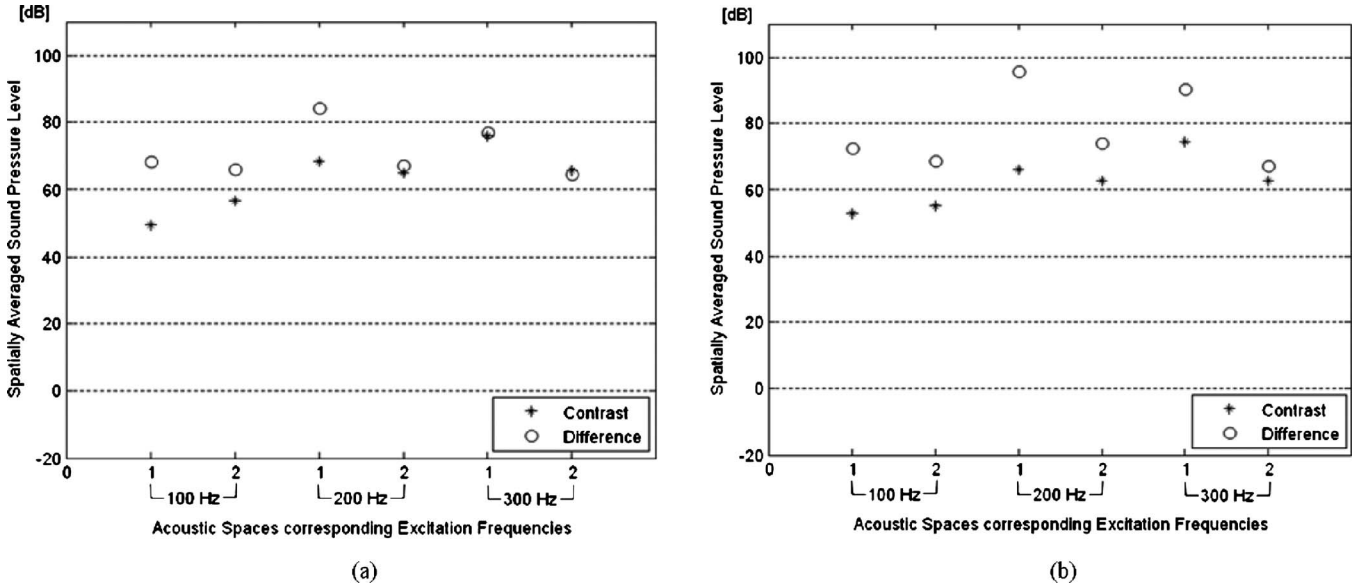

FIG. 10. Spatially averaged measured acoustic pressure levels of two acoustic spaces based on Table IV in (a) circular and (b) spherical arrays (*: contrast control method, °: energy difference maximization method).

tween two adjacent spaces. The proposed method is compared with a previously suggested method for the maximization of acoustic contrast. The relative performance of the methods has been evaluated by using free field monopole simulations and real experiments with a loudspeaker array. Improvements are observed from the previous method on the basis of various performance criteria, such as pressure difference between two acoustic spaces, efficiency of radiation and source strength distribution. In addition, a computational robustness and a reduction in errors are ensured since the method proposed does not include any ill-conditioning problems caused by a matrix inversion and the retrieval of its eigenvalues and eigenvectors from a non-Hermitian matrix. This is especially helpful when the acoustic transfer functions are measured because small measurement errors in the elements of the matrix can cause unexpectedly large errors in the results. Experimental results also show the advantages of the proposed method from the practical point of view. Control sources distributed in the three dimensional structure show better performance that those in the two dimensional case. The proposed method therefore provides a good alternative to the previous method in practical applications.

ACKNOWLEDGMENTS

This work was supported by the Korea Ministry of Knowledge Economy (MKE) (Grant No. 2006-S-006-04) and the IT R&D program of MIC/IITA (Grant No. 2007-S-004-01).

[1]P. A. Nelson and S. J. Elliott, *Active Control of Sound* (Academic, New York, 1992).
[2]D. L. Smith, "Discrete-element line arrays—Their modelling and optimisation," J. Audio Eng. Soc. **45**, 949–964 (1997).
[3]S. Haykin, J. H. Justice, N. L. Owsley, J. L. Yen, and A. C. Kak, *Array Signal Processing* (Prentice-Hall, Englewood Cliffs, NJ, 1985).
[4]W. F. Druyvesteyn and J. Garas, "Personal sound," J. Audio Eng. Soc. **45**, 685–701 (1997).
[5]J. Choi and Y. Kim, "Generation of an acoustically bright zone with an illuminated region using multiple sources," J. Acoust. Soc. Am. **111**, 1695–1700 (2002).
[6]S. J. Elliott and M. Jones, "Active headrest for personal audio," J. Acoust. Soc. Am. **119**, 2702–2709 (2006).
[7]J.-H. Chang, C.-H. Lee, J.-Y. Park, and Y.-H. Kim, "A realization of sound focused personal audio system using acoustic contrast control," J. Acoust. Soc. Am. **125**, 2091–2097 (2009).
[8]C. W. Therrien, *Discrete Random Signals and Statistical Signal Processing* (Prentice-Hall, Englewood Cliffs, NJ, 1992), pp. 685–695.
[9]L. Meirovitch, *Principles and Techniques of Vibrations* (Prentice-Hall, Englewood Cliffs, NJ, 1997), pp. 232–249.
[10]J. S. Arora, *Introduction to Optimum Design* (McGraw-Hill, New York, 1989), pp. 111–136.
[11]G. W. Stewart, *Introduction to Matrix Computations* (Academic, New York, 1973).
[12]J.-H. Chang, M.-H. Song, J.-Y. Park, and Y.-H. Kim, "How does the loudspeaker arrangement affect the personal audio system characteristics?," Proceedings of ICSV16, Krakow, Poland (2009).
[13]F. M. Fazi, P. A. Nelson, J. E. N. Christensen, and J. Seo, "Surround system based on three dimensional sound field reconstruction," Proceedings of the 125th AES Convention, Audio Engineering Society, San Francisco, CA (2008).
[14]F. M. Fazi, V. Brunel, P. A. Nelson, L. Hörchens, and J. Seo, "Measurement and Fourier-Bessel analysis of loudspeaker radiation patterns using a spherical array of microphones," Proceedings of the 124th AES Convention, Audio Engineering Society, Amsterdam (2008).
[15]M. V. Brunel, "Measurement and spherical harmonic representation of loudspeaker radiation pattern," MS thesis, ISVR, University of Southampton, Southampton, United Kingdom, 2007.